Behavioral/Systems/Cognitive

Attentional Facilitation throughout Human Visual Cortex Lingers in Retinotopic Coordinates after Eye Movements

Julie D. Golomb,[1] Alyssa Y. Nguyen-Phuc,[2] James A. Mazer,[1,3,4]* Gregory McCarthy,[1,4]* and Marvin M. Chun[1,3,4]*

[1]Interdepartmental Neuroscience Program, [2]Yale College, [3]Department of Neurobiology, School of Medicine, and [4]Department of Psychology, Yale University, New Haven, Connecticut 06520

With each eye movement, the image of the world received by the visual system changes dramatically. To maintain stable spatiotopic (world-centered) visual representations, the retinotopic (eye-centered) coordinates of visual stimuli are continually remapped, even before the eye movement is completed. Recent psychophysical work has suggested that updating of attended locations occurs as well, although on a slower timescale, such that sustained attention lingers in retinotopic coordinates for several hundred milliseconds after each saccade. To explore where and when this "retinotopic attentional trace" resides in the cortical visual processing hierarchy, we conducted complementary functional magnetic resonance imaging and event-related potential (ERP) experiments using a novel gaze-contingent task. Human subjects executed visually guided saccades while covertly monitoring a fixed spatiotopic target location. Although subjects responded only to stimuli appearing at the attended spatiotopic location, blood oxygen level-dependent responses to stimuli appearing after the eye movement at the previously, but no longer, attended retinotopic location were enhanced in visual cortical area V4 and throughout visual cortex. This retinotopic attentional trace was also detectable with higher temporal resolution in the anterior N1 component of the ERP data, a well established signature of attentional modulation. Together, these results demonstrate that, when top-down spatiotopic signals act to redirect visuospatial attention to new retinotopic locations after eye movements, facilitation transiently persists in the cortical regions representing the previously relevant retinotopic location.

Introduction

An essential function of the visual system is to maintain stable representations of the environment across saccadic eye movements. As the eyes move, the retinotopic (eye-centered) positions of objects change, whereas their spatiotopic (world-centered) positions remain stable. How does the visual system resolve the intrinsic instability of a retinotopic representation in the face of almost continuous eye movements? One idea is that the apparent stability of visual perception is attributable in part to neural "remapping," where the spatial receptive field of a neuron is updated with each saccade, often before the saccade is completed. A remapped neuron may exhibit an anticipatory response before the saccade to a stimulus presented in its future receptive field or it may simply respond to the "memory trace" of that same stimulus once the saccade has brought it into the now-current receptive field (Duhamel et al., 1992; Nakamura and Colby, 2002; Kusunoki and Goldberg, 2003; Merriam et al., 2003; Melcher, 2007; Parks and Corballis, 2008). In both types of remapping, the response is to a stimulus presented before the saccade, even if the response continues after the saccade. Conversely, when stimuli are presented after completion of the saccade, responses are restricted to stimuli appearing in the appropriate, current receptive field location (Kusunoki and Goldberg, 2003).

In a recent psychophysics study, we reported a different effect when sustained, endogenous attention is engaged: when subjects performed a task requiring sustained attention at a spatiotopic location, stimuli presented up to 150 ms after the saccade still revealed behavioral facilitation at the previously relevant retinotopic location (Golomb et al., 2008). This phenomenon, termed the "retinotopic attentional trace," is robust across various experimental manipulations emphasizing spatiotopic over retinotopic representations (Golomb et al., 2010). Importantly, the converse is not true; spatiotopic facilitation is completely absent in tasks emphasizing retinotopic representations (Golomb et al., 2008).

The retinotopic attentional trace is consistent with a neural model in which attentional salience maps operate primarily in a retinotopic reference frame. Topographic maps of visual space have been discovered across various regions of human cortex (Sereno et al., 1995; Engel et al., 1997; Kastner et al., 2007; Saygin and Sereno, 2008), many of which, particularly in occipital cortex, operate in a retinotopic reference frame (Gardner et al., 2008). Many of these visual areas also update their transient visual representations in conjunction with saccades (Medendorp et al., 2003; Merriam et al., 2003, 2007), presumably based on input from efferent oculomotor signals (Sommer and Wurtz, 2006) and/or spatiotopic signals arising from other brain regions (Zipser and Andersen, 1988; Duhamel et al., 1997; Snyder et al.,

Received March 26, 2010; revised June 7, 2010; accepted June 16, 2010.

This research was supported by National Institutes of Health (NIH) Grants EY014193 and P30-EY000785 (M.M.C.), MH05286 (G.M.), and EY018853 (J.A.M.), the Whitehall Foundation (J.A.M.), and a National Science Foundation fellowship and NIH Fellowship MH083374 (J.D.G.). We thank E. Velten for assistance in data collection and A. Leber and N. Turk-Browne for helpful comments and suggestions.

*J.A.M., G.M., and M.M.C. contributed equally to this work.

Correspondence should be addressed to Julie Golomb at her present address: McGovern Institute for Brain Research, Massachusetts Institute of Technology, 77 Massachusetts Avenue, Building 46-4141, Cambridge, MA 02139. E-mail: jgolomb@mit.edu.

DOI:10.1523/JNEUROSCI.1546-10.2010

 0270-6474/10/3010493-14$15.00/0

1998). However, when a locus of endogenous attention must be sustained across a saccade, facilitation built up before the saccade in retinotopically organized areas may take time to decay, resulting in a retinotopic attentional trace of neural facilitation. In this report, we conducted complementary functional magnetic resonance imaging (fMRI) and event-related potential (ERP) studies in human observers to address the question of where and when in the hierarchy of cortical visual processing the retinotopic attentional trace resides.

Materials and Methods

Subjects. Six subjects (five female; mean age, 22.8 years; range, 20–26 years) were included in the fMRI study, and 14 (eight female; mean age, 23.1 years; range, 20–28 years) in the ERP study. All subjects were neurologically intact with normal or corrected-to-normal vision and had extensive experience as psychophysics and eye-tracking subjects; four subjects participated in both studies, and two subjects (J.G., A.N.P.) were also authors. Each fMRI subject participated in multiple scanning sessions (two to six sessions of 1.5–2 h) to obtain extensive data for the main task. Five of the six fMRI subjects were also brought in for one to two additional scanning sessions for more extensive retinotopic mapping (the sixth subject acquired a metal implant and could no longer be scanned; however, sufficient mapping data were acquired during the initial sessions to obtain basic maps).

Each ERP subject participated in a single 2 h session [including electroencephalogram (EEG) and eye-tracker setup time]. One subject who had initial difficulty with the eye tracker was brought back for a second session to obtain enough data. Four additional subjects were recruited for the experiment but excluded from analyses because difficulty with the system setup prevented us from acquiring the full set of data (two subjects) or eye-tracker calibration and/or subject error resulted in insufficient experimental power once error trials (fixation breaks or false-alarm responses) were excluded from analyses (two subjects).

Informed consent was obtained for all subjects, and the study protocols were approved by the Human Investigation Committee of the Yale School of Medicine and the Human Subjects Committee of the Faculty of Arts and Sciences at Yale University.

Experimental setup. Stimuli were generated using the Psychtoolbox extension (Brainard, 1997) for Matlab (MathWorks). During fMRI scanning, stimuli were displayed with a liquid crystal display projector onto a screen mounted in the rear of the scanner bore, which subjects viewed from a distance of 79 cm via a mirror attached to the head coil (maximal field of view, 23.5°). Eye position was monitored using a modified ISCAN eye-tracking system, in which the camera and infrared source were attached to the head coil above the mirror. ERP stimuli were presented on a 19-inch flat-screen cathode ray tube monitor. Subjects were seated at a chinrest positioned 60 cm from the monitor, so that the entire display subtended 32 × 20° visual angle. Eye position was monitored using an ASL 5000 eye-tracking system (Applied Science Laboratories). For both tasks, pupil and corneal reflection (CR) position were recorded at 60 Hz, and gaze angle (pupil-CR) was computed online to obtain accurate timing of saccades for gaze-contingent displays and to ensure that subjects remained fixated (within 1.8° of the fixation dot) during the remainder of the task.

fMRI task and stimuli. Subjects covertly monitored a fixed, centrally positioned spatiotopic location ("target" location) while making guided saccades among four different fixation locations surrounding this central target (Fig. 1). Each trial began with a white fixation dot (0.29° in diameter) that appeared at one of the four possible fixation locations, arranged as the corners of a 9.4° × 9.4° square centered on the spatiotopic target location. On a given trial, subjects either remained fixated at the original location ("no-saccade trials") or made a guided saccade, 9.4° in either the vertical or horizontal direction, to the indicated location ("saccade trials"). All possible fixation and saccade locations were tested an equal number of times, and order was counterbalanced within each block of trials; to minimize the occurrence of non-task-related eye movements, the counterbalancing was done such that every trial began at the fixation location where the previous trial had ended.

To probe attentional topography, Gabor patch stimuli were presented at various delays before and after saccades; subjects were instructed to attend and respond only to stimuli appearing at the spatiotopic target location; stimuli appearing at retinotopic and control nontarget locations were to be ignored. Probe stimuli were high contrast (92%), high spatial frequency (4.75 cycles/°) Gabor patches (Gaussian-modulated sine waves) sized 1.96° × 1.96° ($\sigma = 0.56°$) and oriented 45° to either the left or right of vertical. On each trial, an array of nine randomly oriented probe stimuli appeared simultaneously after a variable delay. The probe and fixation locations were arranged such that a probe always appeared in the central target location, which occupied a different quadrant of the visual field for each fixation location (Fig. 1*a*,*b*, insets). There were no exogenous cues differentiating the target location from the other probe locations, and thus equivalent visual stimulation was provided in all four quadrants at the target eccentricity (6.65°).

Trial progression is illustrated in Figure 1. On saccade trials, the fixation dot remained on the screen for a few seconds before jumping to a new fixation location. Subjects were instructed to immediately saccade to the new fixation location while maintaining attention at the central target location. Eye position was monitored online to obtain sensitive timing of saccade completion; once fixation was successfully acquired at the new location, the probe array was presented after a delay of either 50 ms ("saccade early-delay trials") or 1550 ms ("saccade later-delay trials"). The probe array was presented for 250 ms, immediately followed by an array of identically sized visual masks (plaid Gabors constructed of the sum of the two oriented Gabors) for 250 ms. Subjects were instructed to make an unspeeded two-alternative forced-choice button press to report the orientation (leftward or rightward tilt) of the probe stimulus appearing at the target location. The brief, masked presentation of the probe stimuli required subjects to maintain attention at the target location to successfully perform the task. Saccade and no-saccade trials were intermixed to further ensure that subjects were actively attending to the target location before and after the saccade.

Once the masks were extinguished, the fixation dot dimmed to gray for 18 s to allow the slow event-related hemodynamic response to decay before the next trial. Subjects were allowed to blink during this period but were instructed to otherwise maintain fixation. Each scanning run consisted of 32 trials total, with eight trials each of no-saccade early, no-saccade later, saccade early, and saccade later trial types. Over the course of multiple scanning sessions, each subject completed between 64 and 120 trials per trial type. To ensure accurate fixation and saccade behavior, we analyzed eye traces offline and discarded trials in which subjects fixated for <85% of the trial (indicating fixation breaks beyond normal blinking) or took longer than 600 ms to complete the saccade. The number of rejected trials did not differ across the four trial types ($F < 1$), and the number of remaining trials included in the analysis ranged from 55 to 120 slow event-related trials per condition, per subject.

Gaze-contingent timing of probe delays. As mentioned above, on saccade trials, the probe array was presented after a delay of either 50 ms (saccade early-delay trials) or 1550 ms (saccade later-delay trials) after the saccade. Because we have demonstrated previously that retinotopic facilitation is maximal during the first 50–100 ms after the saccade (Golomb et al., 2008), it was critical to ensure that the early-delay stimuli were presented precisely within this range. We thus time-locked stimulus presentation on each trial to completion of the saccade, as opposed to fMRI image acquisition, to account for trial-to-trial variation in saccadic latency. So that probe stimulus presentation would be as synchronized as possible to fMRI image acquisition, we calculated the subject's average saccadic latency after each block of trials and used this average latency to dynamically adjust trial timing such that completion of the saccade corresponded as closely as possible with the fMRI image acquisition pulse occurring 3 s into the trial.

In other words, if the saccadic latency on a trial was exactly equal to the calculated average, the saccade would be completed at 3000 ms into the trial, and probe stimuli would be presented at 3050 ms for an early-delay trial or 4550 ms for a later-delay trial. In reality, across all included trials, the mean ± SD stimulus onset times were 3079.7 ± 94.3 ms for early delays and 4581.9 ± 53.4 ms for later delays. On no-saccade trials, the fixation dot never moved and the probe array appeared while subjects

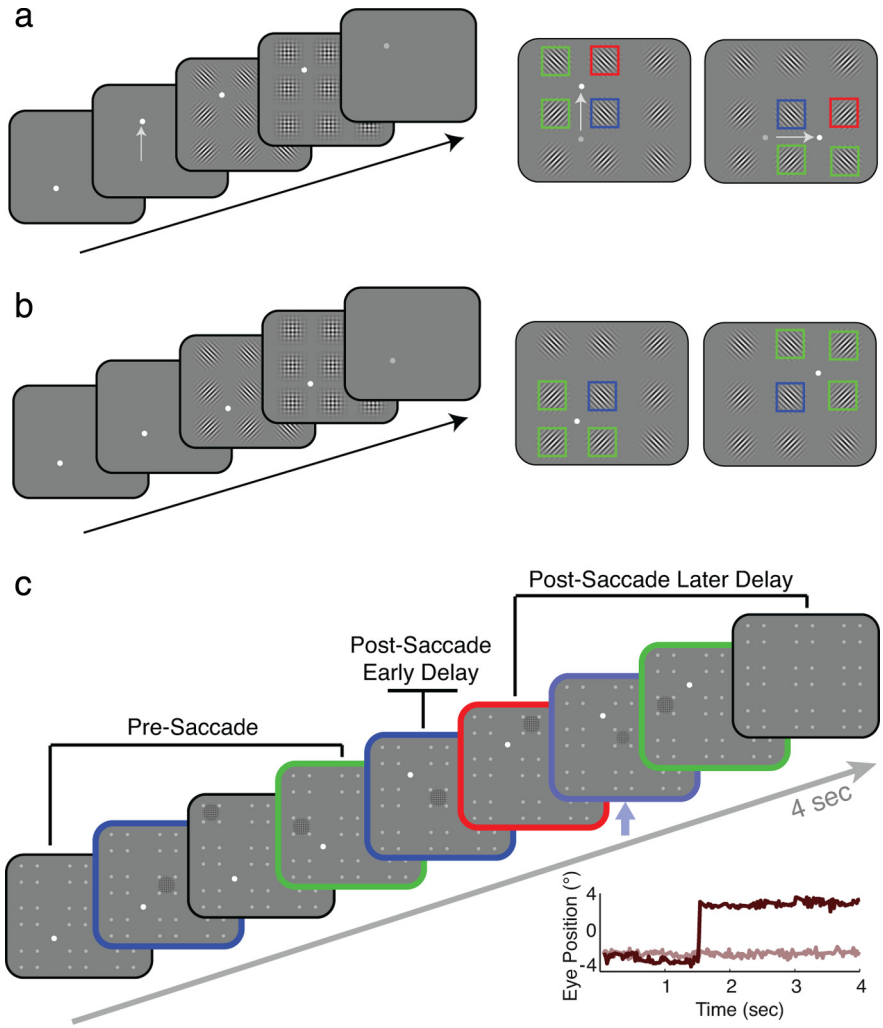

Figure 1. Task design. ***a***, ***b***, fMRI task. Subjects fixated and saccaded between four locations (white dots), while continuously attending to the central target location. ***a***, Saccade trials. After ~3 s of stable fixation, the fixation dot moved to a new location, and subjects executed a single accurate saccade (gray arrow not actually present on screen). After 50 or 1550 ms, an array of Gabor patches appeared simultaneously in the nine locations shown for 250 ms, followed by a 250 ms mask array. Subjects always reported the orientation of the stimulus in the central target location regardless of current fixation position. The four stimuli immediately surrounding the final fixation, corresponding to the four visual field quadrants, were coded according to whether they occupied the spatiotopic (blue), retinotopic (red), or control (green) positions. Different saccade patterns placed these locations in different quadrants for each trial. ***b***, For no-saccade trials, the fixation dot never moved, and subjects remained fixated for either 1.5 or 3 s before the stimuli appeared. The four stimulus quadrants were coded as spatiotopic/retinotopic (blue) or control (green). The fixation dot dimmed for 18 s between trials. ***c***, ERP task. An example 4 s trial is illustrated, with corresponding eye trace below (dark brown is vertical eye position, light brown is horizontal). Subjects fixated the white dot and attended to the central target location. Placeholders demarcating the nine possible stimulus locations were present on the screen at all times (dim gray spots). Stimuli appeared one at a time every 250–550 ms. Subjects pressed a button any time a smaller target stimulus appeared in the target location (light blue arrow). At an unpredictable delay (here ~1.5 s into the trial), the fixation dot jumped to a new location and subjects executed a saccade while continuing to monitor the spatiotopic target location. Stimuli were classified according to delay condition (presaccade, postsaccade early, postsaccade later), and position (spatiotopic, blue; retinotopic, red; control, green). Responses to target stimuli or stimuli appearing at other positions were not analyzed.

were still fixating the original location, at ~1550 ms (no-saccade early trials) and 3050 ms (no-saccade later trials). Stimulus onset time was jittered using the average saccade time to make these trials as similar as possible to the saccade trials; actual stimulus onset times were 1563.2 ± 42.6 and 3058.8 ± 43.3 ms.

fMRI data acquisition and preprocessing. MRI scanning was performed with a Siemens Trio 3 T scanner using an eight-channel receiver array head coil. Functional data was acquired with a T2*-weighted gradient-echo sequence (repetition time, 1500 ms; echo time, 25 ms; flip angle, 80°; matrix, 64 × 64). Twenty-six slices (3 mm thick, 0 mm gap) were taken oriented parallel to the calcarine sulcus to obtain full coverage of occipital and parietal cortex with a 3 mm isotropic voxel resolution. The functional data were coregistered with a T1-weighted anatomical sequence of the same slice orientation acquired during each scanning session and a high-resolution three-dimensional magnetization-prepared rapid-acquisition gradient echo anatomical scan acquired once per subject.

Preprocessing of the data was done using Brain Voyager QX (Brain Innovation). The first six volumes of each functional run were discarded, and the remaining data were corrected for slice acquisition time and head motion, temporally high-pass filtered, and normalized into Talairach space (Talairach and Tournoux, 1988). The high-resolution three-dimensional anatomical images were used to create flattened representations of the cortical surface for each hemisphere, after segmenting the gray and white matter, inflating the cortical sheet, and cutting and unfolding the inflated brain along five segments, including the calcarine sulcus. Data were exported to Matlab (MathWorks) using the Brain Voyager BVQXtools Matlab toolbox, and all subsequent analyses were done in Matlab. Maps were projected back into Brain Voyager for visualization.

Retinotopic mapping and region of interest definition. A combination of retinotopic mapping techniques were used to define the borders of visual areas and select regions of interest (ROIs) for each visual field quadrant within each area (see Fig. 3*a*). Eye position was monitored during all tasks to ensure proper fixation. First, standard rotating wedge and expanding/contracting ring stimuli were used to map polar angle and eccentricity of early visual regions (Engel et al., 1994; Sereno et al., 1995; DeYoe et al., 1996). High-contrast radial checkerboard patterns were presented as 60° wedges or rings and flickered at 4 Hz. Maximal eccentricity was 12°, and the central 1.2° foveal region was not stimulated. Each run rotated clockwise or counterclockwise or expanded or contracted through six cycles with a period of 24 s/cycle. Subjects fixated at the center of the display and pressed a button every time the black fixation dot dimmed to gray. Five subjects completed a minimum of four runs each of the polar angle and eccentricity stimuli. One of the subjects also completed a set of polar angle runs in which covert attention was directed to the rotating wedge, and the subject pressed a button every time one of the checks dimmed to gray. Second, an eccentricity-specific polar angle stimulus was used to restrict stimulation and focus attention at the target eccentricity used in the main task. A colored square of the same size (1.96° × 1.96°) and eccentricity (6.65°) as the main task probe stimuli rotated clockwise or counterclockwise with a period of 24 s for six cycles. The square changed color at a rate of 4 Hz, and subjects were instructed to covertly attend to the rotating square and press a button whenever the square was colored red. All six subjects completed at least four runs of this task.

Data from each technique were analyzed using standard phase-encoded analysis methods: the best-fitting phase and correlation coefficient was obtained for each voxel using Fourier analysis and averaged across clockwise and counterclockwise runs to compensate for hemody-

namic lag. Phase angle maps, thresholded based on correlation coefficient, were displayed on the flattened cortex. Visual field boundaries were defined for visual cortical areas V1, V2, V3, ventral V4, V3A, and V7 following standard phase-reversal criteria (Sereno et al., 1995; DeYoe et al., 1996; Engel et al., 1997; Larsson and Heeger, 2006; Swisher et al., 2007), and eccentricity-specific ROIs were drawn within these areas based on the available combination of retinotopic mapping data for a given subject. Although there has been recent interest in defining V4 to include both dorsal and ventral regions (Hansen et al., 2007), the eccentricity-specific visual field locations of interest for our ROIs seemed to have good coverage of both quadrants contained within ventral V4.

Slow event-related analysis. On each trial of the main task, probe stimuli appeared simultaneously in each visual quadrant. Stimuli were arranged so that spatiotopic, retinotopic, and control locations were all probed on each trial but in different visual quadrants. We thus assigned each visual quadrant a condition code for each trial according to what type of stimulus appeared within that visual quadrant on that trial. For saccade trials, quadrants were coded according to whether they were occupied by the spatiotopic target, the retinotopic nontarget, or one of two control nontargets. Quadrants on no-saccade trials were coded as containing the spatiotopic/retinotopic target or one of three control nontargets. These assignments depended on fixation and saccade position (Fig. 1*a*,*b*, insets); however, across an entire run, each quadrant contained an equal distribution of spatiotopic, retinotopic, and control conditions.

Within each quadrant-based ROI, event-related averages were calculated separately for spatiotopic, retinotopic, and control conditions at early and later probe delays and were represented as percentage signal change relative to the single volume at the start of the trial (before any stimuli appeared). The time courses for each condition were then averaged across quadrants within a given visual area. This resulted in a single average time course for each of the following conditions, for each visual area and subject: (1) no-saccade early: spatiotopic/retinotopic, control; (2) no-saccade later: spatiotopic/retinotopic, control; (3) saccade early: spatiotopic, retinotopic, control; and (4) saccade later: spatiotopic, retinotopic, control.

Statistical analysis. The peak period of the blood oxygen level-dependent (BOLD) response was defined separately for each subject, delay, and visual area by taking the single peak time point and any contiguous time points whose magnitudes were not significantly different from that of the peak. This "statistical peak" method accounts for hemodynamic variations in time-to-peak across subjects and visual areas and is independent of the spatiotopic/retinotopic/control comparison. Once the peak period was identified, the average BOLD response within this period was calculated for the spatiotopic, retinotopic, and control conditions. Peak responses in the control conditions were used as the baseline responses for visual stimulation; control peaks were subtracted from the corresponding retinotopic and spatiotopic peaks for each subject, delay, and region. The resulting retinotopic and spatiotopic peak facilitation were compared using repeated-measures ANOVAs and planned *t* tests. All *t* tests were paired and two tailed. Greenhouse–Geisser corrections were applied to any ANOVA comparisons not meeting the assumption of sphericity.

Event-related potential task and stimuli. The task was similar to the fMRI task, with the timing and stimuli optimized for an ERP-based assessment of visuospatial attention, modeled after ERP investigations of visuospatial attention in the absence of eye movements (Di Russo et al., 2003). To take full advantage of the higher temporal resolution of ERP, stimuli were presented sequentially in rapid succession (i.e., only one stimulus appeared on the screen at a time), while subjects covertly attended to a fixed spatiotopic location (target location) and responded only to targets appearing in this location. Each trial began with the appearance of a white fixation dot (0.19° in diameter) at one of four locations, located at the corners of an imaginary 7.5° × 7.5° square centered on the target location. In the ERP task, each trial lasted 4 s; on each trial, subjects made a single guided 7.5° horizontal or vertical saccade. The saccade cue appeared 1.2–2.8 s (jittered) after the start of the trial; data from trials in which the subject did not accurately saccade to the saccade target within 600 ms were discarded. All possible fixation and saccade locations were tested an equal number of times, and order was counterbalanced within each block of trials; to avoid extraneous eye movements, the counterbalancing was done such that every trial began at the fixation location where the previous trial had ended. To minimize EEG artifacts, subjects were instructed to remain fixated (except for the single saccade) and avoid blinking during the 4 s trial; they were encouraged to blink during the 2 s intertrial interval when the fixation dot dimmed to gray.

During the course of the trial, probe stimuli were presented for 50 ms at stimulus onset asynchronies of 250–550 ms. The stimuli were circular black and white plaid (sum of two sinusoids) patterns that appeared one at a time in a pseudorandom sequence at the nine possible stimulus locations. The stimulus locations were each marked by a placeholder (four small gray dots on the corners of a 2.2° × 2.2° square) continuously visible on the screen; all stimuli appeared within areas denoted by the placeholders. Ninety percent of the stimuli were "standard" stimuli sized 2° in diameter. The remaining 10% were target stimuli sized 1.4–1.6° in diameter. Subjects were instructed to press a button whenever they saw one of the smaller target stimuli appear in the target location. They were instructed to ignore target stimuli that did not appear in that attended location. The size of the target stimuli was adjusted at the beginning of the experiment during a series of practice blocks and if necessary after each block of 24 trials in the main task to keep target detection performance near 75%. ERPs to target stimuli were not analyzed, nor were any other stimuli to which the subject made a false-alarm response.

On each trial, a total of 7–12 stimuli were presented (Fig. 1*c*). Because there was an eye movement on every trial, some stimuli were presented before the eye movement (analogous to no-saccade trials in the fMRI study), and other stimuli were presented after the eye movement (analogous to saccade trials). Any stimulus that was presented before the eye movement was classified as a "presaccade" stimulus. These stimuli ranged from 3000 to 350 ms before the eye movement: no stimuli were presented during the oculomotor planning or execution periods. On each trial, one stimulus was always presented between 25 and 75 ms after completion of the eye movement; this stimulus was coded as the "postsaccade early-delay" stimulus. All stimuli presented at later delays (350–2250 ms after the eye movement) were classified as "postsaccade later-delay" stimuli. Stimuli could appear in spatiotopic, retinotopic, and control locations at all delays. A single control location was chosen for each trial so that eccentricity and spatial uncertainty were equated across the three conditions, although stimuli could also occasionally occur at a none-of-the-above location (not analyzed) to keep the task unpredictable. To further bias subjects to attend to the spatiotopic target location, stimuli were presented in the spatiotopic location more frequently than the other locations (~45% of the time). However, because there was less power for the postsaccade early-delay condition (only one per trial), at this particular delay probe distribution was 33% spatiotopic, 33% retinotopic, and 33% control locations. For each subject, the approximate number of stimuli presented in each condition was as follows: (1) presaccade: 950 spatiotopic/retinotopic, 325 control; (2) postsaccade early: 150 spatiotopic, 150 retinotopic, 150 control; and (3) postsaccade late: 700 spatiotopic, 350 retinotopic, 350 control.

We also incorporated a small percentage of "blank" events into our design to serve as a baseline. Stimulus events were designated to occur every 250–550 ms; however, for ~10% of these events, we did not actually present the stimulus on the screen. These "blank" trials were intended to dissociate stimulus response from saccade response, especially for the early-delay stimuli whose ERPs would otherwise be contaminated with activity associated with saccade execution. These blank trials were matched for time relative to the saccade, and ERPs to the corresponding blank events were subtracted from the ERPs for the stimulus events.

Electroencephalogram recording and processing. EEG was recorded simultaneously from 32 scalp locations using tin electrodes embedded in a fabric cap (Electrode Caps International). The electrode locations included the 10/20 system, as well as the electrooculogram (EOG) recorded from two electrodes attached beside each eye and one underneath the right eye. Scalp electrodes were referenced to a single electrode placed on the participant's nose. Signals were amplified (gain of 20,000) and bandpass filtered (0.1–100 Hz) by an EEG amplifier. The impedance of each electrode on the electro-cap was below 5 kΩ.

The EEG was continuously sampled at 250 Hz and logged to a disk file using custom software. Digital codes corresponding to stimulus condition were written to a separate digital channel that was sampled simultaneously with the EEG. A 1–50 Hz digital bandpass filter was applied offline to eliminate line noise and slow drift from the recorded EEG.

Event-related potential analysis. For each subject, each standard stimulus was coded according to the following factors: (1) position: spatiotopic, retinotopic, control, other; (2) delay: presaccade, postsaccade early-delay, postsaccade later delays; (3) quadrant: upper left, upper right, lower left, lower right; and (4) saccade direction: right, left, up, down. Blank events were coded as additional conditions according to delay and saccade direction. Stimuli to which the subject falsely responded or stimuli that appeared on trials on which subjects were not properly fixated or saccading were coded as errors and excluded from additional analyses. On average, 11.6% of trials were excluded; this did not vary significantly across delays or positions.

Epochs beginning 100 ms before and extending to 500 ms after the appearance of each standard stimulus (or the equivalent for blank trials) were extracted from the continuous EEG. Although most eye movements would have already been excluded in the previous step, epochs with EOG artifacts (indicating eye blinks) were also discarded using the variance of the EOG channels as criteria. The mean amplitude of the 100 ms interval before stimulus onset was subtracted from every time point of the epoch to remove any prestimulus EEG baseline differences, and the artifact-free epochs were averaged separately for each condition.

For each stimulus condition ERP, the corresponding blank condition ERP (matched for saccade direction and delay) was subtracted to create a difference ERP. Difference ERPs were averaged across quadrants and saccade directions to obtain ERPs for spatiotopic, retinotopic, and control conditions at each of the three delay periods for each subject. For secondary analyses, data were subdivided by hemisphere and by horizontal/vertical saccade direction. Neither hemisphere nor saccade direction affected the overall pattern of results, so the main analyses focus on the collapsed data.

ERPs for each condition were grand-averaged across subjects (mean of means), and particular ERP components known to be modulated by attention (Awh et al., 2000; Di Russo et al., 2003) were characterized (supplemental Table S1, available at www.jneurosci.org as supplemental material). To simplify statistical analyses, we conducted comparisons on a single characteristic electrode for each attention-related component: Oz for the P1 and posterior N1 components, and Cz for the anterior N1 component. The average amplitude of each peak at its characteristic electrode was measured for each subject, and planned *t* tests (paired, two-tailed) were conducted comparing spatiotopic and retinotopic conditions to the control condition.

Results

fMRI experiment

The fMRI study was designed to take advantage of the well established topographical organization of visual cortex by presenting stimuli simultaneously in all four visual quadrants. Retinotopic mapping was used to create quadrant-based ROIs, and stimulus responses within each ROI were coded as spatiotopic, retinotopic, or control based on eye position at the time of the stimulus onset (Fig. 1*a*,*b*). Response data were then collapsed across quadrants to generate pooled spatiotopic, retinotopic, and control time courses. This design both maximized experimental power, because we obtained spatiotopic, retinotopic, and control responses on every trial, and equated bottom-up visual stimulation across experimental conditions. Thus, any differences in the BOLD response between conditions are entirely attributable to the locus of top-down attention. Moreover, these differences should reflect the observer's attentional state at the time of stimulus presentation. That is, although the BOLD response to a stimulus presented 50 ms after a saccade will not manifest for several seconds as a result of the intrinsic temporal dynamics of the hemodynamic response, the magnitude of the delayed response should be greater for retinotopic versus control stimuli in areas exhibiting a retinotopic attentional trace. In these same areas, the delayed BOLD response to a stimulus presented 1550 ms after the saccade should show only task-relevant spatiotopic facilitation, assuming that the temporary retinotopic attentional trace has decayed by the later stimulus onset time. Conversely, regions containing spatiotopically organized salience maps should exhibit purely task-relevant spatiotopic facilitation at both delays.

fMRI task behavior

Behavioral performance on the fMRI task is shown in supplemental Table S2 (available at www.jneurosci.org as supplemental material). Because of technical difficulties, button-press responses were not recorded for a portion of trials (randomly interspersed) for the first few subjects and sessions. Of the responses that were recorded, subjects correctly discriminated the orientation of the spatiotopic target with 91.6 ± 6.5% accuracy (mean ± SD). Discrimination accuracy was 90.0% for no-saccade trials and 93.2% for saccade trials, illustrating that subjects were clearly capable of maintaining the spatiotopic task-relevant location after the eye movement. Reaction time was significantly slower to spatiotopic targets appearing immediately after a saccade versus well after a saccade ($t_{(5)} = 4.62$, $p = 0.006$), which could reflect that attention was still in the process of updating at the early delay. However, because there was no behavioral response to the retinotopic and control stimuli (subjects always only responded to the spatiotopic target), this slowing could also be attributable to an overall difficulty processing all stimuli immediately after a saccade and should not be taken as conclusive evidence for the retinotopic attentional trace.

Overall fixation percentage was 91.8%, and the mean saccadic latency was 336.8 ms. Trials in which subjects stayed fixated <85% of the time or had a saccadic latency >600 ms were excluded from fMRI analyses.

Attentional modulation in area V4

To look for evidence of the retinotopic attentional trace in human visual cortex, we initially focused on area V4, which has long been recognized as both retinotopically organized (Gattass et al., 1988; Sereno et al., 1995) and a major target of top-down attentional modulation (Moran and Desimone, 1985; Tootell et al., 1998) in both humans and monkeys. In addition, the position of V4 as a convergence point of bottom-up and top-down processing streams makes it a plausible candidate area for a dynamic salience map (Mazer and Gallant, 2003; Ungerleider et al., 2008).

To ensure that our new paradigm was effective at successfully directing spatial attention to the target location, we first examined BOLD responses in V4 to stimuli appearing in the absence of an eye movement. We observed clear attentional modulation of responses to stimuli appearing in attended (spatiotopic/retinotopic) versus unattended (control) locations at both delays probed on no-saccade trials (Fig. 2*a*,*b*). To quantify attentional facilitation (Fig. 2*e*), we computed the peak facilitation for each position, delay, and subject by calculating the peak magnitude of the BOLD response for spatiotopic/retinotopic conditions and subtracting the peak magnitude for the corresponding control condition (representing baseline visual stimulation). Across the six subjects, significant attentional facilitation was found at the spatiotopic/retinotopic position for both the early and late no-saccade delays ($t_{(5)} = 3.24$, $p = 0.023$ and $t_{(5)} = 3.28$, $p = 0.022$, respectively).

Given that V4 activity accurately reflects the presence of an attentional locus at the task-relevant location in the absence of

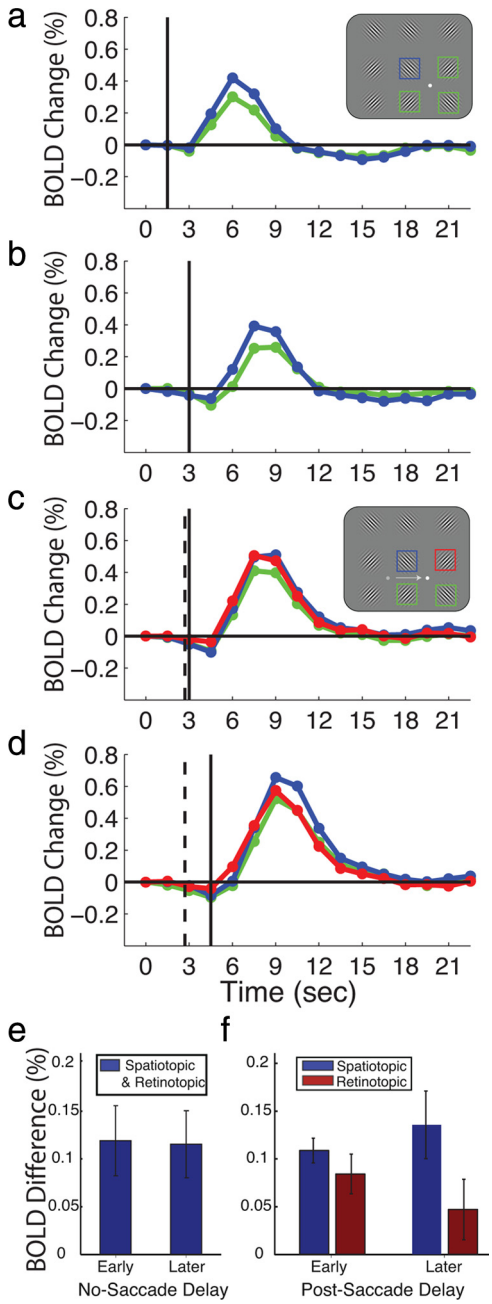

Figure 2. V4 time courses and peak activation. Solid black line indicates stimulus presentation, and dotted black line is saccade time. ***a***, ***b***, No-saccade trials. Blue is the response to the spatiotopic/retinotopic target stimulus, and green is the response to control nontarget. ***a***, No-saccade early. ***b***, No-saccade later. ***c***, ***d***, Saccade trials. Blue is response to spatiotopic target, red to retinotopic nontarget, and green to control nontarget. ***c***, Saccade early (stimulus 50 ms after saccade completion). ***d***, Saccade later (stimulus 1550 ms after saccade completion). ***e***, Peak facilitation for retinotopic and spatiotopic positions compared with control; error bars are SEM ($n = 6$).

saccades, the critical question is how V4 represents this attentional locus after a saccade. We compared BOLD responses for the spatiotopic target, retinotopic nontarget, and control nontarget stimuli presented immediately after the saccade (Fig. 2*c*) versus those presented well after the saccade (Fig. 2*d*). In area V4, there was a significant position (spatiotopic, retinotopic) × delay (early, later) interaction ($F_{(1,5)} = 9.33$, $p = 0.028$). At the early delay (50 ms after saccade completion), both task-relevant spatiotopic and task-irrelevant retinotopic facilitation were significant ($t_{(5)} = 8.38$, $p < 0.001$ and $t_{(5)} = 4.05$, $p = 0.010$, respectively). At 1.5 s later, only task-relevant spatiotopic targets remained significantly facilitated ($t_{(5)} = 3.83$, $p = 0.012$); V4 responses to task-irrelevant retinotopic stimuli were no longer significantly different from control stimulation ($t_{(5)} = 1.48$, $p = 0.199$). This pattern provides neural evidence for the retinotopic attentional trace in human visual cortex, specifically in extrastriate area V4. When a spatiotopic location is task relevant and stimuli are presented well after the eye movement, only responses to stimuli at the attended spatiotopic location show facilitation. In contrast, responses to stimuli appearing immediately after the eye movement show facilitation at both the spatiotopic and retinotopic locations, suggesting that, although attention has successfully updated to compensate for the saccade, residual facilitation remains at the now irrelevant retinotopic location for some time.

The main effect of delay was not significant ($F < 1$), but there was a significant main effect of position ($F_{(1,5)} = 23.03$, $p = 0.005$), with spatiotopic facilitation generally exceeding retinotopic facilitation. The fact that the task-relevant spatiotopic facilitation was so reliable after the saccade attests to the subjects' successful performance and effort in this task. It may also reflect the fact that, in contrast to previous tasks (Golomb et al., 2008, 2010), subjects here were forced to respond to the spatiotopic stimulus (and nothing else) on every trial, making the retinotopic stimuli truly task irrelevant. Consequently, it is perhaps not surprising that subjects exhibited stronger, more reliable spatiotopic facilitation. It is notable that, despite this very strong behavioral bias toward spatiotopic representations, V4 still showed clear attentional effects at the retinotopic location immediately after the saccade.

Facilitation in other visual areas

A similar pattern of facilitation was observed across all of the occipital regions localized via retinotopic mapping (Fig. 3). In all of these areas, task-relevant spatiotopic facilitation grew with increasing postsaccade delay, whereas task-irrelevant retinotopic facilitation declined. An omnibus 6 × 2 × 2 (region × delay × position) ANOVA revealed a main effect of region ($F_{(1,5)} = 3.52$, $p = 0.046$) but no significant region × delay ($F_{(1,5)} = 2.42$, $p = 0.11$) or region × position ($F < 1$) interactions. Critically, the delay × position interaction found in V4 remained significant in the larger ANOVA ($F_{(1,5)} = 10.44$, $p = 0.023$) and was not modulated by region ($F < 1$), suggesting that the retinotopic attentional trace found in V4 may be a common feature of early, ventral, and dorsal visual processing streams.

To further investigate potential effects of region that may have been obscured by the omnibus ANOVA, we classified individual regions according to whether they were early (V1/V2/V3), ventral (V4), or dorsal (V3A/V7). Again we found a significant delay × position interaction ($F_{(1,5)} = 11.44$, $p = 0.020$) that was not significantly modulated by region ($F < 1$). Furthermore, in all three types of regions, there was significant attentional facilitation at the task-irrelevant retinotopic location immediately after the eye movement (early, $t_{(5)} = 2.99$, $p = 0.030$; ventral, $t_{(5)} = 4.05$, $p = 0.010$; dorsal, $t_{(5)} = 3.20$, $p = 0.024$).

Time course of facilitation

The above analyses were based on enhancement of the peak stimulus response as a measure of attentional facilitation, but examination of the details of the BOLD time courses reveals interesting additional information. Although both spatiotopic and retinotopic positions showed significant peak facilitation for the saccade early-

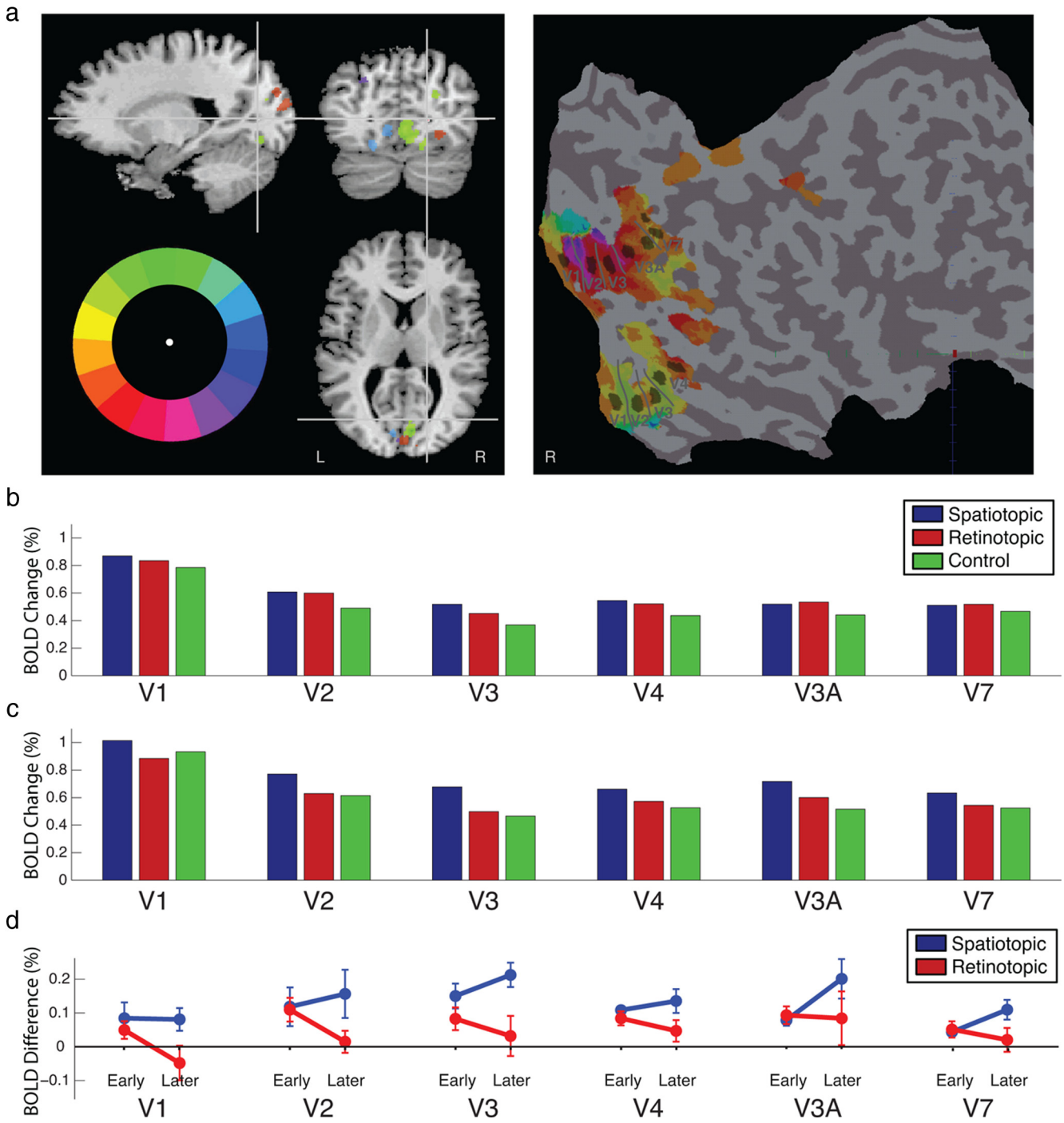

Figure 3. Occipital ROIs and activation. ***a***, ROIs for a representative subject. Left, Areas V1–V7 color coded according to quadrant, based on the visual field legend at the bottom left. ROIs were restricted to the target eccentricity used in the main task. Right, Sample flat map for the right hemisphere. Combined activation map from all retinotopic mapping runs is displayed colored according to the same legend. ROIs are drawn on top of the activation map. ***b***, ***c***, Peak activation for spatiotopic, retinotopic, and control stimuli for areas V1–V7. ***b***, Saccade early delay. ***c***, Saccade later delay. ***d***, Peak facilitation for retinotopic and spatiotopic positions (compared with control) for early and late delays; error bars are SEM ($n = 6$).

delay stimuli, retinotopic facilitation was more pronounced earlier in the time course, whereas spatiotopic facilitation dominated later. To explore these differences, we computed the time courses of facilitation in V4, by subtracting the control BOLD response at each point in time from the spatiotopic and retinotopic responses (Fig. 4).

At the temporal resolution of the BOLD response, spatiotopic facilitation appears locked to stimulus onset for both postsaccade delays, peaking ~4–6 s after stimulus presentation. In contrast, retinotopic facilitation peaked earlier for both delays. This pattern could reflect the fact that attention was initially at the retinotopic location in both cases and subsequently had to be updated to the spatiotopic location to correctly perform the task. Sustaining attention at a particular spatial location can result in a shift in baseline facilitation even in the absence of a stimulus (Kastner et al., 1999). If this baseline facilitation reflects an increase in the spontaneous firing rate of neurons representing the attended location (Luck et al., 1997) and the salience map still reflects the old retinotopic location right after the eye movement,

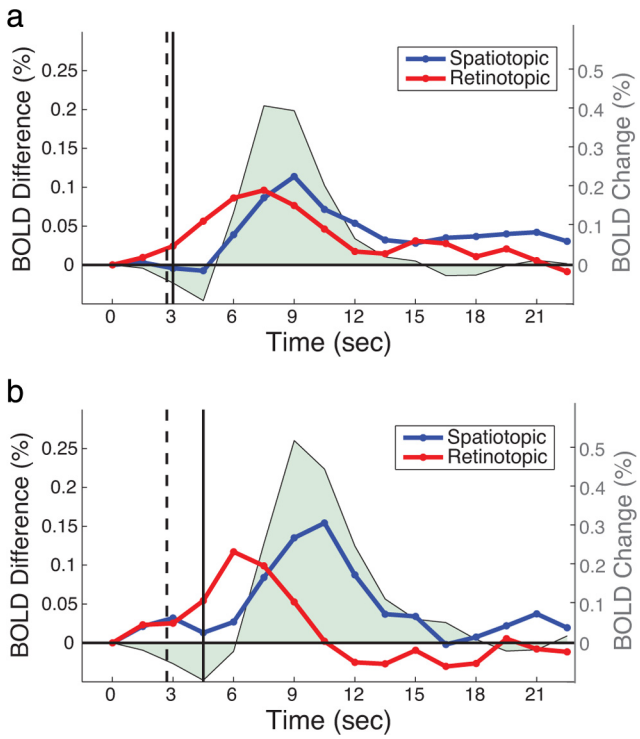

Figure 4. Time course of facilitation, V4. Spatiotopic and retinotopic facilitation (difference from control) at each time point. A magnitude of zero means no difference from control, and positive values reflect attentional facilitation. BOLD time course for control stimulation superimposed in background (right axis). Solid black line indicates stimulus onset, and dotted line indicates saccade time. ***a***, Saccade early delay. ***b***, Saccade later delay. $n = 6$.

then we would expect to see some degree of baseline retinotopic facilitation after the eye movement for both delays. For the early-delay trials, the stimuli are presented during this lingering period, which also results in an enhanced stimulus response at the retinotopic location, whereas at the later delay, stimulus presentation occurs after the trace has dissipated, so only spatiotopic stimuli are enhanced.

It is important to note that, as with all fMRI effects, baseline facilitation is subject to hemodynamic delays. Thus, it is possible that this baseline facilitation could simply be a delayed hemodynamic response reflecting the presaccadic attentional state (which would fall in this same retinotopic quadrant) as opposed to an actual retinotopic attentional trace. If this were the case and retinotopic facilitation was only attributable to the presaccadic state, we would expect the retinotopic time course of facilitation to be identical for both delays. The fact that facilitation is larger and persists longer for the earlier versus later delay suggests something above and beyond hemodynamically delayed presaccadic facilitation, in other words, a retinotopic attentional trace reflecting residual neural facilitation after the eye movement. Although the limited temporal resolution of fMRI prevents us from conclusively dissociating these neural and hemodynamic components, in the following section, we use the substantially higher temporal resolution of ERP to avoid hemodynamic confounds and selectively investigate neural contributions to the retinotopic attentional trace.

ERP experiment

To take advantage of the higher temporal resolution of ERP, we modified the fMRI task so that stimuli were presented individually in rapid sequence, again while subjects monitored and responded only to targets appearing at the spatiotopic location. As in the fMRI task, we classified each stimulus presentation as spatiotopic, retinotopic, or control and presaccadic, early postsaccadic, or late postsaccadic based on the subject's eye position and timing of the stimulus onset relative to saccades (Fig. 1*c*). This approach is similar to that used in the pioneering ERP studies of Di Russo et al. (2003) investigating visuospatial attention in the absence of eye movements, in which attention typically enhances the P1 (occipital electrodes, latency of 100–150 ms), anterior N1 (frontocentral electrodes, latency of 140–150 ms), and posterior N1 (occipitoparietal electrodes, latency of 170–200 ms) ERP components.

ERP task behavior

To characterize target detection performance, we calculated the A' score, an index of signal detection sensitivity ranging from 0 to 1, where 0.5 is chance discrimination and 1 is perfect performance (Grier, 1971). The size of the target stimulus relative to standard stimuli was adjusted for each subject to achieve a hit rate of 70–75%, ensuring that the task would be sufficiently challenging to require effortful allocation of attention to the target location. The mean ± SD A' score across subjects was 0.92 ± 0.03, confirming that subjects were successfully performing the challenging target detection task. Detection performance was actually better for spatiotopic targets presented after the saccade than before (supplemental Table S3, available at www.jneurosci.org as supplemental material), illustrating that subjects were clearly capable of maintaining the spatiotopic task-relevant location after the eye movement. Performance was significantly worse for postsaccade early-delay targets than later-delay targets ($t_{(13)} = -4.56$, $p = 0.001$), but as in the fMRI experiment, this does not necessarily imply that attention was allocated elsewhere. Mean ± SD reaction time to targets was 672.0 ± 61.2 ms. Reaction times did not significantly vary with delay ($F < 1$).

Overall fixation percentage for the included subjects was 89.9 ± 5.3% (mean ± SD), and the mean ± SD saccadic latency was 365.7 ± 40.3 ms.

Difference ERPs

ERPs from individual stimuli were pooled based on when (presaccade, postsaccade early, postsaccade later) and where (spatiotopic, retinotopic, control) the stimulus appeared and then averaged across the 14 subjects. The raw ERPs for the postsaccade early-delay conditions were contaminated with large, but consistent, voltage deflections resulting from the saccade (supplemental Fig. S1, available at www.jneurosci.org as supplemental material). These artifacts were removed by subtracting a saccade-only ERP response recorded on blank trials (i.e., no visual stimulus) from each raw stimulus-evoked ERP to obtain difference ERPs. The difference ERPs for the postsaccade early events closely resemble those of the other delays (see Fig. 8), although there is clearly more noise at this delay; this is likely attributable to the fact that there were fewer postsaccade early events to average, although incomplete removal of eye movement artifacts by the differencing procedure could also contribute to this noise. All subsequent analyses were performed on the difference ERPs (referred to simply as ERPs from this point forward). Voltage maps for presaccade, postsaccade early, and postsaccade later stimuli are displayed in Figures 5–7, and ERP waveforms for all electrodes can be found in supplemental Figures S2–S4 (available at www.jneurosci.org as supplemental material). To quantify attentional modulation for the P1, anterior N1, and posterior N1 components, we focused analyses on the Oz and Cz electrodes

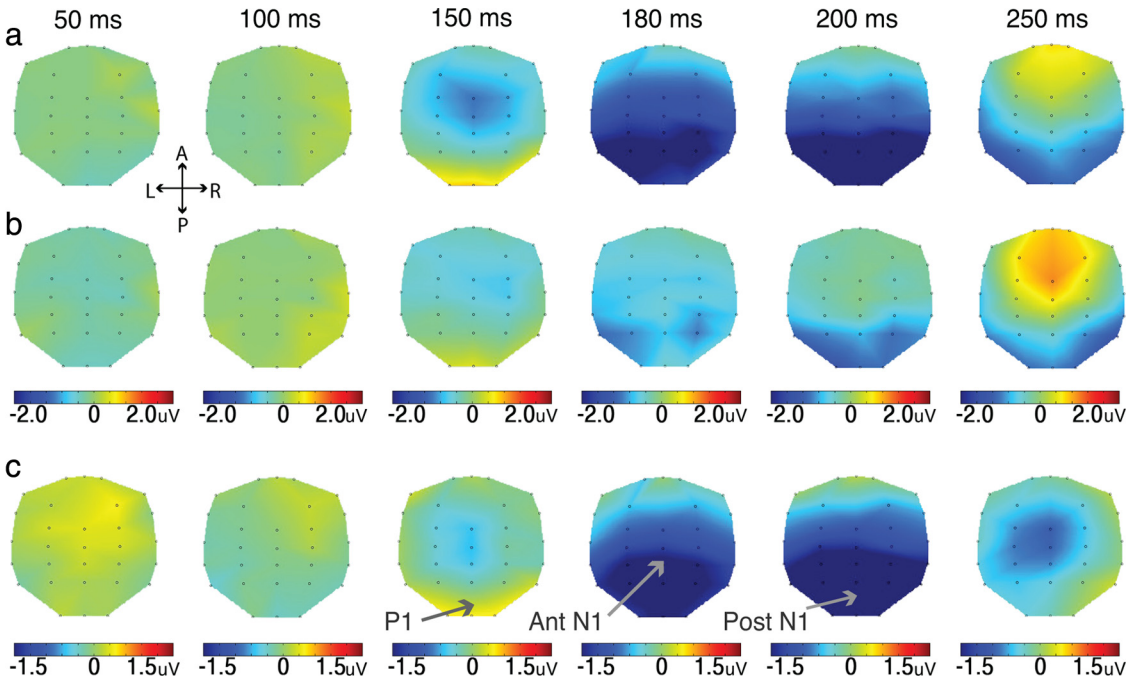

Figure 5. ERP voltage maps over time for presaccade stimuli. ***a***, ***b***, Grand-averaged ERP voltage maps at specified time points after presentation of a stimulus in the attended spatiotopic/retinotopic location (***a***) and unattended control location (***b***). ***c***, Difference activity (spatiotopic/retinotopic − control) over the same time period. Electrode locations are depicted on a top-down view of the skull, oriented according to the anterior/posterior (A/P) and left/right (L/R) axes pictured. Attentionally modulated P1, anterior N1, and posterior N1 components are labeled with arrows. $n = 14$.

(supplemental Table S1, available at www.jneurosci.org as supplemental material). Attentional modulation of each component is illustrated in Figure 8 and discussed below in order of latency.

P1 component

The P1 component was identified at a peak latency of 128–144 ms at the occipitoparietal electrodes. In the presaccade ERPs (i.e., when the visual stimulus appeared before initiation of the guided saccade), the amplitude of the P1 component was significantly enhanced for stimuli appearing in attended (spatiotopic/retinotopic) compared with control locations ($t_{(13)} = 2.20$, $p = 0.047$). For both early and later postsaccade delays, the P1 was enhanced at both retinotopic and spatiotopic positions, although this difference only reached statistical significance at later delays (later: $t_{(13)} = 3.00$, $p = 0.010$ and $t_{(13)} = 2.34$, $p = 0.036$ for spatiotopic and retinotopic, respectively; early: $t_{(13)} = 0.86$, $p = 0.406$ and $t_{(13)} = 1.85$, $p = 0.087$ for spatiotopic and retinotopic, respectively). There were few events in the saccade early-delay conditions, and thus this comparison was underpowered (see Materials and Methods) compared with the presaccade or postsaccade later conditions. It is therefore not surprising that attentional modulation might be more difficult to observe in this condition, particularly for the P1 component, which was the smallest in magnitude of the three components.

Anterior N1 component

The anterior N1 component was found on frontocentral electrodes with a peak latency of 168–188 ms. This component was significantly modulated by attention in the presaccade conditions ($t_{(13)} = -4.47$, $p = 0.001$). For the postsaccade early delays, significant modulation was found for stimuli appearing in both the task-relevant spatiotopic position ($t_{(13)} = -2.77$, $p = 0.016$) and the task-irrelevant retinotopic position ($t_{(13)} = -3.04$, $p = 0.010$). In contrast, at later delays, significant anterior N1 modulation was found only for the task-relevant spatiotopic position ($t_{(13)} = -3.13$, $p = 0.008$); stimuli presented in the retinotopic position were no longer significantly facilitated over control stimuli ($t_{(13)} = 0.43$, $p = 0.675$). This pattern is consistent with the previously reported behavioral pattern of facilitation (Golomb et al., 2008) and provides more neural evidence in support of the retinotopic attentional trace. This result is even stronger than the behavioral and fMRI data, because the ERP task was maximally biased toward forcing observers to maintain and use spatiotopic representations. The task required constant attention to the spatiotopic location: observers responded only to targets at the spatiotopic location, there were repeated presentations of stimuli at the spatiotopic location, and spatiotopic landmarks were continuously visible on the screen throughout the experiment (Fig. 1*c*). Nevertheless, during the first 75 ms after the eye movement, residual retinotopic facilitation at the anterior N1 component was just as strong as the task-relevant spatiotopic facilitation.

Posterior N1 component

The posterior N1 component was detectable across a similar set of occipitoparietal electrodes as the P1 component at a peak latency of 196–204 ms. Significant attentional modulation of the posterior N1 component was found in the presaccade conditions ($t_{(13)} = -4.93$, $p < 0.001$). At postsaccade delays, the pattern of posterior N1 modulation was quite different from the anterior N1 pattern; at both early and late delays, the posterior N1 was only facilitated for task-relevant spatiotopic stimuli. Spatiotopic attentional facilitation was significant at the later delays ($t_{(13)} = -3.10$, $p = 0.008$) and displayed a trend at early delays ($t_{(13)} = -1.56$, $p = 0.143$), whereas posterior N1 responses to retinotopic stimuli were not significantly enhanced over controls at either delay ($t_{(13)} = 0.89$, $p = 0.392$ and $t_{(13)} = 0.53$, $p = 0.607$ for early and later, respectively). If anything, the retinotopic posterior N1 seemed suppressed relative to control. The purely task-relevant nature of this component, especially in light of the anterior N1 results, could reflect that (1) the different components reflect

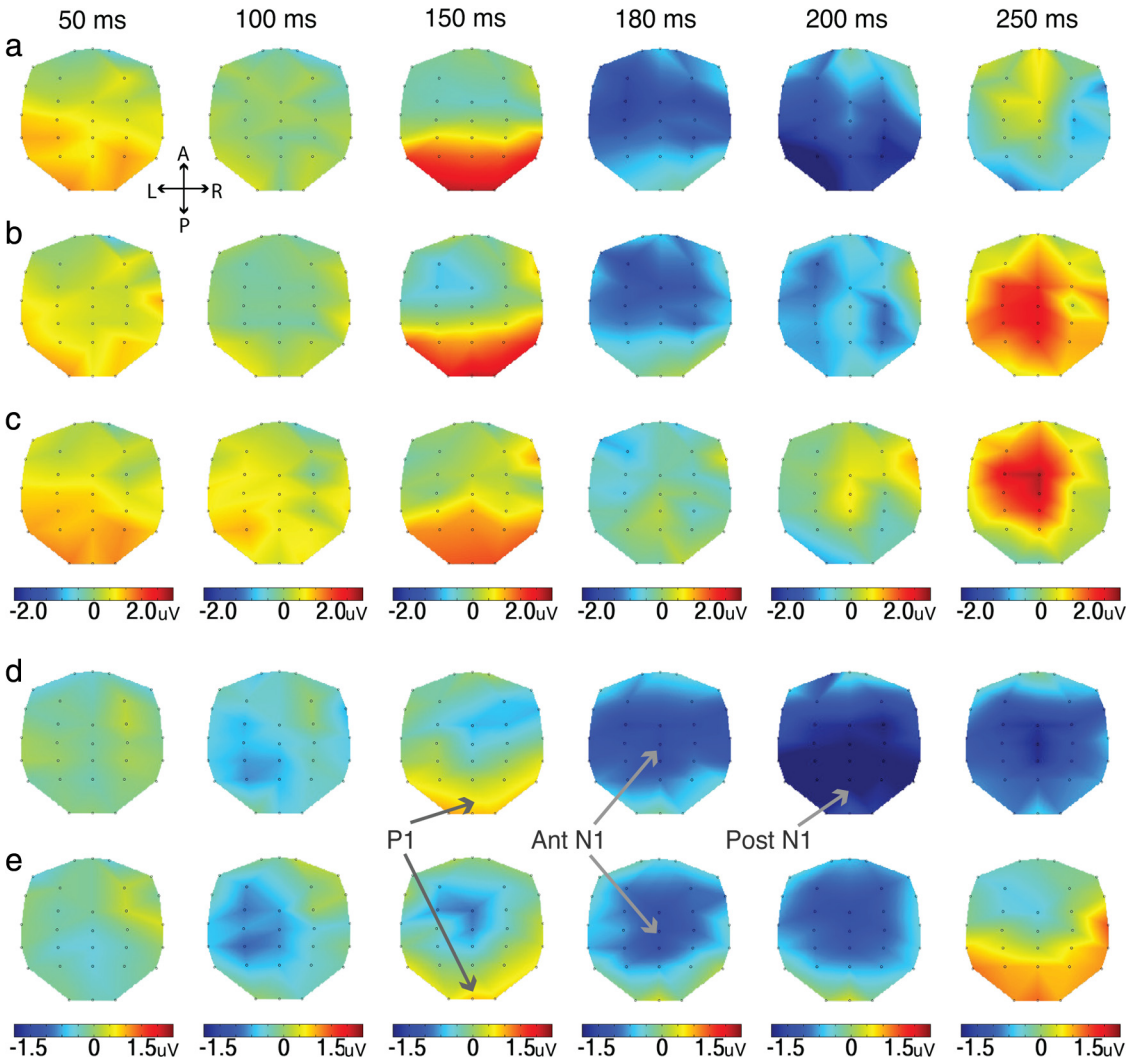

Figure 6. ERP voltage maps over time for postsaccade early-delay stimuli. ***a–c***, Grand-averaged ERP voltage maps at specified time points after presentation of a stimulus in the spatiotopic (***a***), retinotopic (***b***), and control (***c***) locations. ***d***, ***e***, Difference activity relative to control over the same time period. ***d***, Spatiotopic– control. ***e***, Retinotopic– control. Electrode locations are depicted on a top-down view of the skull, oriented according to the anterior/posterior (A/P) and left/right (L/R) axes pictured. Attentionally modulated P1, anterior N1, and posterior N1 components are labeled with arrows. $n = 14$.

different neural processes, and/or (2) the attentional representations captured by this component had already been successfully updated by this point in time.

The differences between ERP components and the implications of such differences for the neural mechanisms of spatial attention in general warrant additional investigation. Perhaps the anterior N1 component occurs at an optimal latency to capture the retinotopic attentional trace, with the earlier P1 component displaying more retinotopic tendencies, and the later posterior N1 component capturing only task-relevant spatiotopic modulation, a latency difference that parallels the different time courses of facilitation in the fMRI study. Alternatively, differences in ERP components may arise from their different neural sources. The study by Di Russo et al. (2003) on which our ERP task was modeled used dipole source localization methods to suggest that the P1 and posterior N1 components originate in extrastriate occipital cortex and the anterior N1 component in superior parietal cortex, near the intraparietal sulcus (IPS). This association is somewhat surprising given that parietal cortex is typically thought of as a candidate area for encoding spatiotopic representations (Zipser and Andersen, 1988; Duhamel et al., 1997; Snyder et al., 1998), and there have been several reports of a progression from retinotopic to increasingly spatiotopic visual representations (in the absence of sustained attention) moving from V1 to higher-order areas (Andersen et al., 1997; Melcher and Colby, 2008; Wurtz, 2008). However, the presence of spatiotopic information does not preclude retinotopic organization, which parietal cortex is also known to contain (Sereno et al., 2001; Medendorp et al., 2003; Silver et al., 2005; Swisher et al., 2007; Gardner et al., 2008; Konen and Kastner, 2008; Saygin and Sereno, 2008; Silver and Kastner, 2009). Our findings of retinotopic attentional traces throughout visual cortex, including area V7, sometimes known as IPS0 (Swisher et al., 2007; Silver and Kastner, 2009), suggest that lingering retinotopic salience maps may extend beyond occipital regions, and parietal and frontal attentional areas will be important regions to explore in future study.

Discussion

The fMRI and ERP data reported here reveal remarkably similar patterns of attentional topography after an eye movement. The experimental task was designed to force subjects to sustain attention at a specific spatiotopic location. Subjects needed to constantly moni-

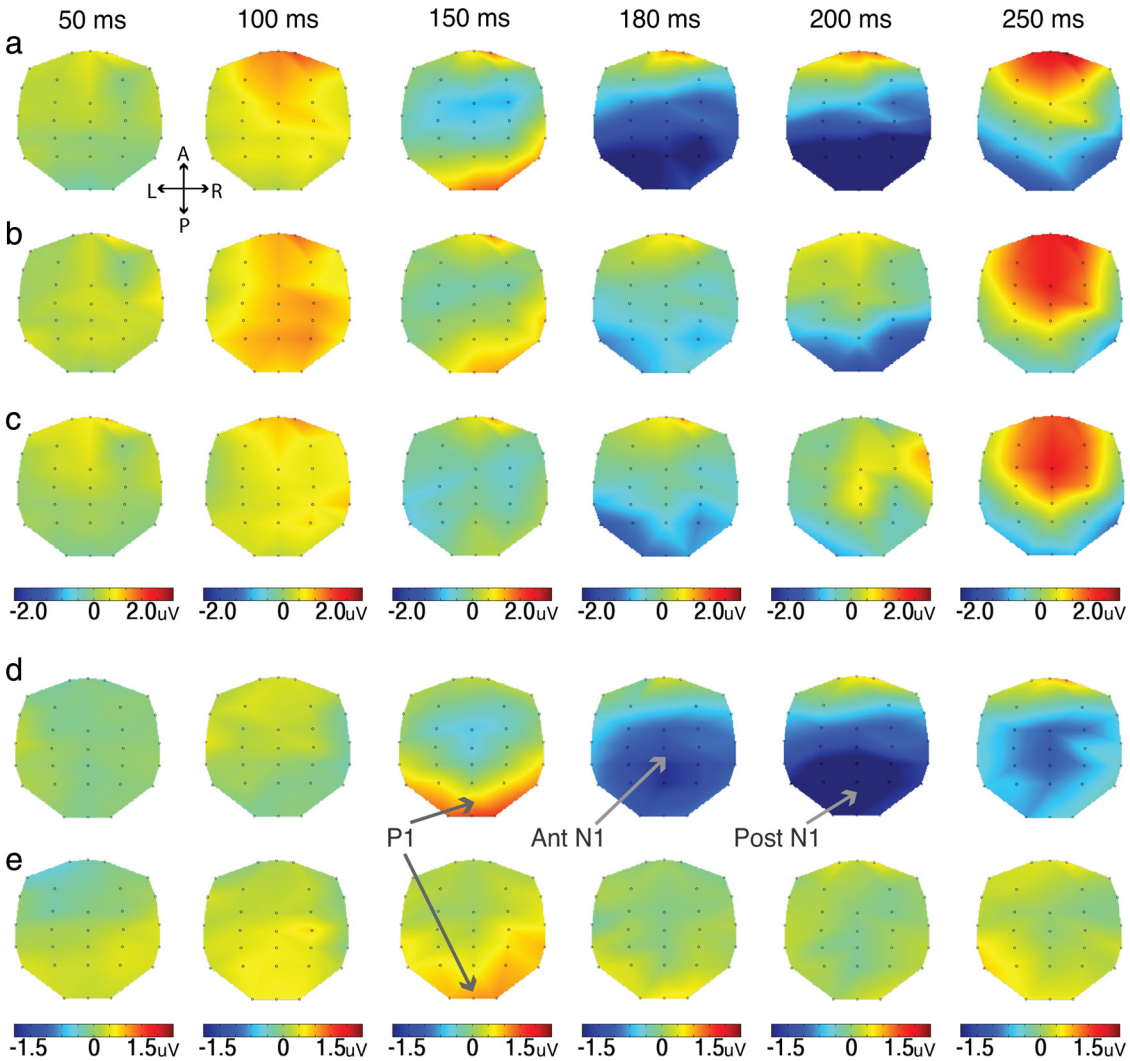

Figure 7. ERP voltage maps over time for postsaccade later-delay stimuli. ***a–c***, Grand-averaged ERP voltage maps at specified time points after presentation of a stimulus in the spatiotopic (***a***), retinotopic (***b***), and control (***c***) locations. ***d***, ***e***, Difference activity relative to control over the same time period. ***d***, Spatiotopic– control. ***e***, Retinotopic– control. Electrode locations are depicted on a top-down view of the skull, oriented according to the anterior/posterior (A/P) and left/right (L/R) axes pictured. Attentionally modulated P1, anterior N1, and posterior N1 components are labeled with arrows. $n = 14$.

tor the spatiotopic location because (1) they did not know when the target stimuli would appear, and (2) the task was sufficiently difficult (because of brief presentation times, visual masking, and near-threshold differences) that successful task performance was critically dependent on accurate allocation of spatiotopic attention. Furthermore, subjects were required to respond only to stimuli appearing in this attended spatiotopic location while ignoring any other stimuli present. The attentional manipulation was clearly successful in both tasks; in the absence of an eye movement, both fMRI and ERP responses were enhanced for stimuli appearing in the attended versus unattended locations. After the saccade was executed, we report two key findings. First of all, neural responses were facilitated at the task-relevant spatiotopic location. Second, spatiotopic facilitation was accompanied by behaviorally inappropriate facilitation at the previous retinotopic location. The former finding, although expected given the strong spatiotopic task emphasis, is also an important confirmation that attention can be sustained across saccades (cf. Hoffman and Subramaniam, 1995; Kowler et al., 1995; Deubel and Schneider, 1996) and successfully remapped to maintain stability (Duhamel et al., 1992). Because we did not present any stimuli immediately preceding or during the saccade, it is unclear whether attentional remapping to the spatiotopic location was anticipatory, although a recent behavioral study has suggested that attention may be predictively remapped (Mathôt and Theeuwes, 2010).

Regardless of when the new spatiotopic location becomes facilitated, it seems to occur before attention has pulled away from the retinotopic location. This delayed transition is consistent with studies involving the switching of attention between two locations while the eyes are fixated (Khayat et al., 2006). The critical difference between these tasks is what causes the reorganization, In the current task, there is no explicit "switch" in the attentional focus: subjects must maintain attention at a particular location, which they perceive to be stable across the saccade. The fact that facilitation lingers at the retinotopic location after the saccade demonstrates that salience maps throughout visual cortex must be actively updated, although the conscious percept is one of instantaneous stability. It is also of note that, although a retinotopic attentional trace exists for a spatiotopically attended location, there is no analogous spatiotopic attentional trace when the retinotopic location is task relevant (Golomb et al., 2008).

Our previous studies have revealed a behavioral retinotopic attentional trace using psychophysical methods (Golomb et al.,

2008, 2010). The fMRI and ERP data reported here provide converging neural evidence and suggest several putative cortical sources for the trace. The fMRI experiment offers neural evidence that the retinotopic attentional trace is instantiated in several different areas of human visual cortex and suggests that attentional maps throughout visual cortex must be dynamically updated after eye movements. The ERP data corroborate the neural basis of attentional updating, with the strongest correlate of the retinotopic attentional trace evident in the anterior N1 component. In addition to providing neural correlates of a behavioral phenomenon, these data further extend the robust nature of the retinotopic attentional trace across different tasks. Retinotopic attentional traces are found when attention is allocated to a spatiotopic location through rehearsal in spatial working memory (Golomb et al., 2008), delayed ocuolomotor planning (Golomb et al., 2010), and constant spatial monitoring (current task).

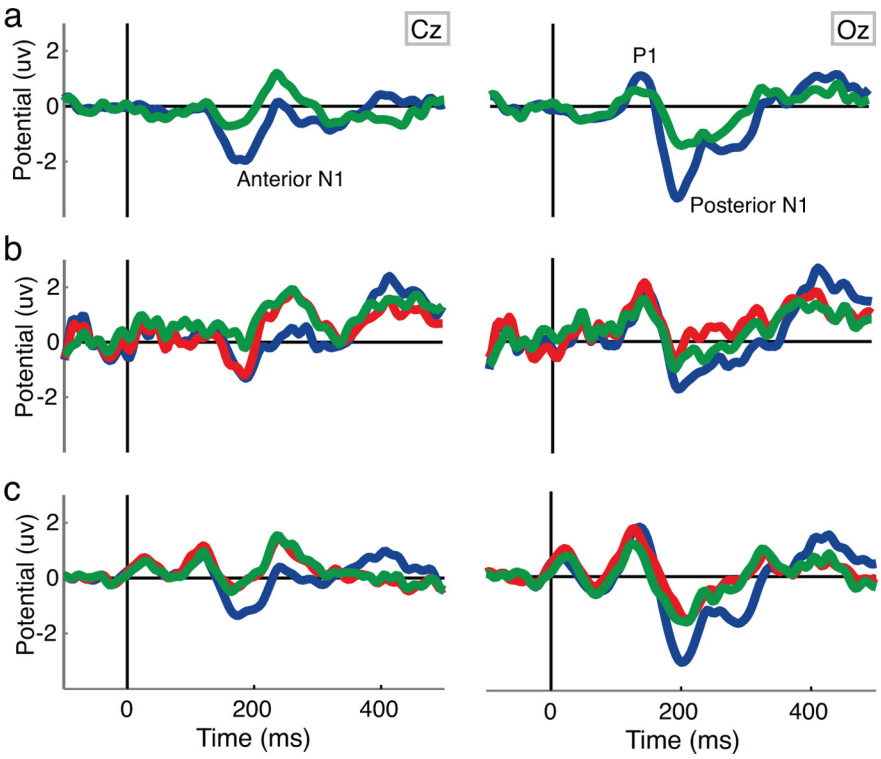

Figure 8. ERPs at characteristic electrodes reflecting P1, anterior N1, and posterior N1 components. Components labeled near peak latency. ***a***, Attentional modulation for presaccade stimuli (blue, spatiotopic/retinotopic; green, control). ***b***, Attentional modulation for postsaccade early-delay stimuli (blue, spatiotopic; red, retinotopic; green, control). ***c***, Attentional modulation for postsaccade later stimuli (blue, spatiotopic; red, retinotopic; green, control). $n = 14$.

This delayed spatial updating, epitomized by the retinotopic attentional trace, may indicate a difference in neural processes involved in maintaining exogenous versus endogenous maps of visuospatial attention (Corbetta and Shulman, 2002). In both cases, spatial updating of retinotopically organized maps involves two complementary processes: remapping to a new location and deactivation or decay at the old location. Kusunoki and Goldberg (2003) demonstrated that, for basic visual (exogenous) responses, these two processes generally occur during the same time period, which is often, but not always, completed in advance of the saccade. Although not all neurons show predictive remapping, stimuli presented after the saccade never evoke inappropriate retinotopic responses (Kusunoki and Goldberg, 2003). In other words, there is a difference between a response to a stimulus presented before the eye movement that persists after the saccade and a response evoked by a stimulus actually presented after the eye movement.

Most previous remapping studies have focused on how the representation of a stimulus presented before a saccade is remapped to the new location. The current investigation focuses on stimuli presented after the saccade, finding consistent evidence for remapped spatiotopic representations, as well as an irrelevant retinotopic representation that is not immediately invalidated. The previous studies demonstrating spatiotopic remapping in fMRI (Merriam et al., 2003, 2007) and ERP (Parks and Corballis, 2008) did not test the retinotopic location immediately after the saccade. Based on other electrophysiology studies that did present stimuli at this location after the saccade and did not evoke responses (Duhamel et al., 1992; Nakamura and Colby, 2002; Kusunoki and Goldberg, 2003; Sommer and Wurtz, 2006), we might expect the retinotopic attentional trace to only emerge when sustained visuospatial attention is involved. Thus, irrelevant distracters may transiently capture attention (Bisley and Goldberg, 2006; Goldberg et al., 2006) and be updated to the relevant spatiotopic location rapidly (Gottlieb et al., 1998), with no residual effects at the retinotopic location. Conversely, an endogenously sustained representation may also update to the spatiotopic location rapidly, but because attentional modulation has built up at the retinotopic location, presumably by engaging reverberatory circuits (Wang, 2001) and synchronous activity (Tallon-Baudry et al., 1998; Fries et al., 2001; Pesaran et al., 2002), the previous retinotopic representation takes time to decay. Consequently, attentional updating is not truly complete until well after the eye movement has been executed.

Thus, we might expect to see two distinct loci of attention around the time of saccade: a quickly remapped spatiotopic locus and a slower decaying retinotopic locus. Our attentional facilitation results for both the fMRI and ERP experiments display this pattern, and the differences between retinotopic and spatiotopic time courses of facilitation provide additional evidence for two distinct mechanisms. This idea is consistent with demonstrations of both spatiotopic and retinotopic components of inhibition of return (Posner and Cohen, 1984; Sapir et al., 2004) and, in particular, the finding that, when the parietal cortex is damaged or impaired, inhibition of return does not remap to the new spatiotopic location, instead remaining in retinotopic coordinates (Sapir et al., 2004; van Koningsbruggen et al., 2010). Perhaps these distinct mechanisms are analogous to findings with neural synchronization and spatial updating, in which it has been suggested that gamma-band synchrony updates faster than alpha-band synchrony (Van Der Werf et al., 2008). Moreover, a related dissociation exists in the infant development literature, in which acquisition of retinotopic representations precedes spatiotopic representations (Gilmore and Johnson, 1997; Kaufman et al., 2006).

Our results suggest that all of the visual regions measured here contain primarily retinotopically organized attentional salience maps that must be dynamically updated when the eyes move to maintain task-relevant spatiotopic representations. If attentional

maps in visual cortex are all retinotopically organized, the updating signal has to come from spatiotopic maps or signals that exist elsewhere in the brain. Spatiotopic representations have been described in parts of parietal cortex (Duhamel et al., 1997; Snyder et al., 1998), although the existence of explicit spatiotopic topography has not been proven. It is also possible that this updating is based purely on corollary discharge signals related to the eye movement itself, and the saccade vector is fed directly to visual cortex allowing maps to update (Matin, 1986; Bridgeman et al., 1994; Sommer and Wurtz, 2006, 2008; Wurtz, 2008). Retinal factors have also been hypothesized to provide the updating signal, through comparison of successive views with respect to a visual reference point, such as the saccade target (McConkie and Currie, 1996; Currie et al., 2000) or other consistent visual information (Deubel et al., 1998; Khayat et al., 2004). Aside from the source of the updating signal, an open question raised by this work is whether the updating signal is simultaneously fed to salience maps throughout visual cortex or whether it originates in one area and propagates forward or backward along the visual stream.

Evidence from our psychophysical, fMRI, and ERP studies now provide converging evidence for a lingering retinotopic attentional trace. When a locus of visuospatial attention must be sustained across an eye movement, residual facilitation transiently remains in cortical areas representing the previous retinotopic location, regardless of compelling top-down signals redirecting attention to the proper task-relevant location. It remains to be seen what benefit such a delayed updating process might offer for visual stability. One possibility is that the retinotopic attentional trace does not actually represent a behavioral benefit but rather provides insight into an imperfect solution our visual systems have developed to optimize computational efficiency and performance in a world where location information is both important and ever-changing.

References

Andersen RA, Snyder LH, Bradley DC, Xing J (1997) Multimodal representation of space in the posterior parietal cortex and its use in planning movements. Annu Rev Neurosci 20:303–330.

Awh E, Anllo-Vento L, Hillyard SA (2000) The role of spatial selective attention in working memory for locations: evidence from event-related potentials. J Cogn Neurosci 12:840–847.

Bisley JW, Goldberg ME (2006) Neural correlates of attention and distractibility in the lateral intraparietal area. J Neurophysiol 95:1696–1717.

Brainard DH (1997) The psychophysics toolbox. Spat Vis 10:433–436.

Bridgeman B, Van der Heijden AHC, Velichkovsky BM (1994) A theory of visual stability across saccadic eye movements. Behav Brain Sci 17:247–257.

Corbetta M, Shulman GL (2002) Control of goal-directed and stimulus-driven attention in the brain. Nat Rev Neurosci 3:201–215.

Currie CB, McConkie GW, Carlson-Radvansky LA, Irwin DE (2000) The role of the saccade target object in the perception of a visually stable world. Percept Psychophys 62:673–683.

Deubel H, Schneider WX (1996) Saccade target selection and object recognition: evidence for a common attentional mechanism. Vision Res 36:1827–1837.

Deubel H, Bridgeman B, Schneider WX (1998) Immediate post-saccadic information mediates space constancy. Vision Res 38:3147–3159.

DeYoe EA, Carman GJ, Bandettini P, Glickman S, Wieser J, Cox R, Miller D, Neitz J (1996) Mapping striate and extrastriate visual areas in human cerebral cortex. Proc Natl Acad Sci U S A 93:2382–2386.

Di Russo F, Martínez A, Hillyard SA (2003) Source analysis of event-related cortical activity during visuo-spatial attention. Cereb Cortex 13:486–499.

Duhamel JR, Colby CL, Goldberg ME (1992) The updating of the representation of visual space in parietal cortex by intended eye movements. Science 255:90–92.

Duhamel JR, Bremmer F, BenHamed S, Graf W (1997) Spatial invariance of visual receptive fields in parietal cortex neurons. Nature 389:845–848.

Engel SA, Rumelhart DE, Wandell BA, Lee AT, Glover GH, Chichilnisky EJ, Shadlen MN (1994) fMRI of human visual cortex. Nature 369:525.

Engel SA, Glover GH, Wandell BA (1997) Retinotopic organization in human visual cortex and the spatial precision of functional MRI. Cereb Cortex 7:181–192.

Fries P, Reynolds JH, Rorie AE, Desimone R (2001) Modulation of oscillatory neuronal synchronization by selective visual attention. Science 291:1560–1563.

Gardner JL, Merriam EP, Movshon JA, Heeger DJ (2008) Maps of visual space in human occipital cortex are retinotopic, not spatiotopic. J Neurosci 28:3988–3999.

Gattass R, Sousa AP, Gross CG (1988) Visuotopic organization and extent of V3 and V4 of the macaque. J Neurosci 8:1831–1845.

Gilmore RO, Johnson MH (1997) Body-centered representations for visually-guided action emerge during early infancy. Cognition 65:B1–B9.

Goldberg ME, Bisley JW, Powell KD, Gottlieb J (2006) Saccades, salience and attention: the role of the lateral intraparietal area in visual behavior. Prog Brain Res 155:157–175.

Golomb JD, Chun MM, Mazer JA (2008) The native coordinate system of spatial attention is retinotopic. J Neurosci 28:10654–10662.

Golomb JD, Pulido VZ, Albrecht AR, Chun MM, Mazer JA (2010) Robustness of the retinotopic attentional trace after eye movements. J Vis 10:19.1–19.12.

Gottlieb JP, Kusunoki M, Goldberg ME (1998) The representation of visual salience in monkey parietal cortex. Nature 391:481–484.

Grier JB (1971) Nonparametric indexes for sensitivity and bias: computing formulas. Psychol Bull 75:424–429.

Hansen KA, Kay KN, Gallant JL (2007) Topographic organization in and near human visual area V4. J Neurosci 27:11896–11911.

Hoffman JE, Subramaniam B (1995) The role of visual attention in saccadic eye movements. Percept Psychophys 57:787–795.

Kastner S, Pinsk MA, De Weerd P, Desimone R, Ungerleider LG (1999) Increased activity in human visual cortex during directed attention in the absence of visual stimulation. Neuron 22:751–761.

Kastner S, DeSimone K, Konen CS, Szczepanski SM, Weiner KS, Schneider KA (2007) Topographic maps in human frontal cortex revealed in memory-guided saccade and spatial working-memory tasks. J Neurophysiol 97:3494–3507.

Kaufman J, Gilmore RO, Johnson MH (2006) Frames of reference for anticipatory action in 4-month-old infants. Infant Behav Dev 29:322–333.

Khayat PS, Spekreijse H, Roelfsema PR (2004) Correlates of transsaccadic integration in the primary visual cortex of the monkey. Proc Natl Acad Sci U S A 101:12712–12717.

Khayat PS, Spekreijse H, Roelfsema PR (2006) Attention lights up new object representations before the old ones fade away. J Neurosci 26:138–142.

Konen CS, Kastner S (2008) Representation of eye movements and stimulus motion in topographically organized areas of human posterior parietal cortex. J Neurosci 28:8361–8375.

Kowler E, Anderson E, Dosher B, Blaser E (1995) The role of attention in the programming of saccades. Vision Res 35:1897–1916.

Kusunoki M, Goldberg ME (2003) The time course of perisaccadic receptive field shifts in the lateral intraparietal area of the monkey. J Neurophysiol 89:1519–1527.

Larsson J, Heeger DJ (2006) Two retinotopic visual areas in human lateral occipital cortex. J Neurosci 26:13128–13142.

Luck SJ, Chelazzi L, Hillyard SA, Desimone R (1997) Neural mechanisms of spatial selective attention in areas V1, V2, and V4 of macaque visual cortex. J Neurophysiol 77:24–42.

Mathôt S, Theeuwes J (2010) Evidence for the predictive remapping of visual attention. Exp Brain Res 200:117–122.

Matin L (1986) Visual localization and eye movements. In: Handbook of perception and human performance (Boff KR, Kaufman L, Thomas JP, eds), pp 20.1–20.45. New York: Wiley.

Mazer JA, Gallant JL (2003) Goal-related activity in V4 during free viewing visual search. Evidence for a ventral stream visual salience map. Neuron 40:1241–1250.

McConkie GW, Currie CB (1996) Visual stability across saccades while viewing complex pictures. J Exp Psychol Hum Percept Perform 22:563–581.

Medendorp WP, Goltz HC, Vilis T, Crawford JD (2003) Gaze-centered updating of visual space in human parietal cortex. J Neurosci 23:6209–6214.

Melcher D (2007) Predictive remapping of visual features precedes saccadic eye movements. Nat Neurosci 10:903–907.

Melcher D, Colby CL (2008) Trans-saccadic perception. Trends Cogn Sci 12:466–473.

Merriam EP, Genovese CR, Colby CL (2003) Spatial updating in human parietal cortex. Neuron 39:361–373.
Merriam EP, Genovese CR, Colby CL (2007) Remapping in human visual cortex. J Neurophysiol 97:1738–1755.
Moran J, Desimone R (1985) Selective attention gates visual processing in the extrastriate cortex. Science 229:782–784.
Nakamura K, Colby CL (2002) Updating of the visual representation in monkey striate and extrastriate cortex during saccades. Proc Natl Acad Sci U S A 99:4026–4031.
Parks NA, Corballis PM (2008) Electrophysiological correlates of presaccadic remapping in humans. Psychophysiology 45:776–783.
Pesaran B, Pezaris JS, Sahani M, Mitra PP, Andersen RA (2002) Temporal structure in neuronal activity during working memory in macaque parietal cortex. Nat Neurosci 5:805–811.
Posner MI, Cohen Y (1984) Components of visual orienting. In: Attention and performance X (Bouma H, Bouwhuis D, eds), pp 531–556. Hillsdale, NJ: Erlbaum.
Sapir A, Hayes A, Henik A, Danziger S, Rafal R (2004) Parietal lobe lesions disrupt saccadic remapping of inhibitory location tagging. J Cogn Neurosci 16:503–509.
Saygin AP, Sereno MI (2008) Retinotopy and attention in human occipital, temporal, parietal, and frontal cortex. Cereb Cortex 18:2158–2168.
Sereno MI, Dale AM, Reppas JB, Kwong KK, Belliveau JW, Brady TJ, Rosen BR, Tootell RB (1995) Borders of multiple visual areas in humans revealed by functional magnetic resonance imaging. Science 268:889–893.
Sereno MI, Pitzalis S, Martinez A (2001) Mapping of contralateral space in retinotopic coordinates by a parietal cortical area in humans. Science 294:1350–1354.
Silver MA, Kastner S (2009) Topographic maps in human frontal and parietal cortex. Trends Cogn Sci 13:488–495.
Silver MA, Ress D, Heeger DJ (2005) Topographic maps of visual spatial attention in human parietal cortex. J Neurophysiol 94:1358–1371.
Snyder LH, Grieve KL, Brotchie P, Andersen RA (1998) Separate body- and world-referenced representations of visual space in parietal cortex. Nature 394:887–891.
Sommer MA, Wurtz RH (2006) Influence of the thalamus on spatial visual processing in frontal cortex. Nature 444:374–377.
Sommer MA, Wurtz RH (2008) Visual perception and corollary discharge. Perception 37:408–418.
Swisher JD, Halko MA, Merabet LB, McMains SA, Somers DC (2007) Visual topography of human intraparietal sulcus. J Neurosci 27:5326–5337.
Talairach J, Tournoux P (1988) Co-planar stereotaxic atlas of the human brain: 3-dimensional proportional system: an approach to cerebral imaging. New York: Thieme.
Tallon-Baudry C, Bertrand O, Peronnet F, Pernier J (1998) Induced gamma-band activity during the delay of a visual short-term memory task in humans. J Neurosci 18:4244–4254.
Tootell RB, Hadjikhani N, Hall EK, Marrett S, Vanduffel W, Vaughan JT, Dale AM (1998) The retinotopy of visual spatial attention. Neuron 21:1409–1422.
Ungerleider LG, Galkin TW, Desimone R, Gattass R (2008) Cortical connections of area V4 in the macaque. Cereb Cortex 18:477–499.
Van Der Werf J, Jensen O, Fries P, Medendorp WP (2008) Gamma-band activity in human posterior parietal cortex encodes the motor goal during delayed prosaccades and antisaccades. J Neurosci 28:8397–8405.
van Koningsbruggen MG, Gabay S, Sapir A, Henik A, Rafal RD (2010) Hemispheric asymmetry in the remapping and maintenance of visual saliency maps: a TMS study. J Cogn Neurosci 22:1730–1738.
Wang XJ (2001) Synaptic reverberation underlying mnemonic persistent activity. Trends Neurosci 24:455–463.
Wurtz RH (2008) Neuronal mechanisms of visual stability. Vision Res 48:2070–2089.
Zipser D, Andersen RA (1988) A back-propagation programmed network that simulates response properties of a subset of posterior parietal neurons. Nature 331:679–684.